Understanding the Structural Properties of a Homologous Series of Bis-diphenylphosphine Oxides

Patrizia Calcagno, Benson M. Kariuki, Simon J. Kitchin, James M. A. Robinson, Douglas Philp,* and Kenneth D. M. Harris*[a]

Abstract: A homologous series of bis-diphenylphosphine oxides $(C_6H_5)_2PO(CH_2)_nPO(C_6H_5)_2$ (with $n = 2-8$; denoted **2**–**8**] have been investigated to explore the effects of a range of competing and cooperative intermolecular and intramolecular interactions on the structural properties in the solid state. The important factors influencing the structural properties include intramolecular aspects such as the conformation of the aliphatic chain and the intramolecular interaction between the two P=O dipoles in the molecule, and intermolecular aspects such as long-range electrostatic interactions (dominated by the arrangement of the P=O dipoles), C–H···O interactions, C–H···π interactions and π···π interactions. Compounds **3** and **5** could be crystallized only as solvate co-crystals (**3**·water and **5**·$(toluene)_2$], whereas the crystal structures of all the other compounds contain only the bis-diphenylphosphine oxide molecule. The crystal structures have been determined from single-crystal X-ray diffraction data, with the exception of **7** (which has been determined here from powder X-ray diffraction data) and **4** (which was known previously). The compounds with even *n* represent a systematic structural series, exhibiting characteristic, essentially linear P=O···P=O···P=O dipolar arrays, together with C–H···O and C–H···π interactions. For the compounds with odd *n*, on the other hand, uniform structural behaviour is not observed across the series, although certain aspects of these crystal structures contribute in a general sense to our understanding of the structural properties of bis-diphenylphosphine oxides. Importantly, for the compounds with odd *n*, there is "frustration" with regard to the molecular conformation, as the preferred all-*anti* conformation of the aliphatic chain gives rise to an unfavourable parallel alignment of the two P=O dipoles within the molecule. Clearly the importance of avoiding a parallel alignment of the P=O dipoles becomes greater as *n* decreases. Local structural aspects (investigated by high-resolution solid-state ^{31}P NMR spectroscopy) and thermal properties of the bis-diphenylphosphine oxide materials are also reported.

Keywords: phosphine oxides · solid-state structures · structure elucidation · structural rationalization

Introduction

The molecular packing arrangements observed in crystals are the outcome of a balance among several different non-covalent forces, which may represent varying degrees between cooperativity and competition.[1–5] In order to understand the optimal structural arrangements observed in crystals, which correspond to minima in total energy, we require an understanding of the interplay between short-range intermolecular forces (such as hydrogen bonding, dispersion and repulsion) that act between functional groups, longer range electrostatic interactions, and intramolecular (conformational) energies. The presence of certain functional groups can lead to predictable local interactions, which may promote characteristic crystal packing motifs in one-, two- and perhaps even three-dimensions. In this regard, the use of hydrogen bonding as a basis for the design and construction of crystals has been particularly exploited.[6–17] Electrostatic interactions, which are significant over long range, may also be an important determinant of the overall packing arrangements observed in crystals. Understanding the structural properties of molecular crystals is further complicated if the molecule in question has intramolecular degrees of freedom, in which case the molecular conformation must also be considered directly in rationalizing the crystal structure. In this regard, we emphasize that the optimal crystal structure does not necessarily contain the molecule in the conformation that is optimal for the isolated molecule—the observed crystal structure represents an overall compromise between several competing and cooperating

[a] Dr. D. Philp, Prof. Dr. K. D. M. Harris, P. Calcagno, Dr. B. M. Kariuki, Dr. S. J. Kitchin, J. M. A. Robinson
School of Chemistry
University of Birmingham
Edgbaston, Birmingham B15 2TT (UK)
Fax: (+44) 121-414-7473
E-mail: D.Philp@bham.ac.uk
K.D.M.Harris@bham.ac.uk

  0947-6539/00/0613-2338 $ 17.50+.50/0

factors, including the intramolecular (conformational) energy and the energies of the different types of intermolecular interactions discussed above.

In seeking to understand the role played by intramolecular and intermolecular factors in controlling crystal packing arrangements, there is continuing interest in the properties of phosphine oxides. The P=O group in phosphine oxides is a good hydrogen-bond acceptor, and phosphine oxides are well known to form complexes in solution[18, 19] and in the solid state.[11, 12, 20–31] In this context, triphenylphosphine oxide (TPPO) has been used[24] to facilitate co-crystal formation, based on the ability of the P=O group to form strong hydrogen bonds to "guest" molecules. Although attempts to rationalize molecular crystal structures are often focused entirely on the nature of short-range interactions between neighbouring molecules, longer range electrostatic interactions may also play a significant role for molecules with large multipole moments. In this regard, the strong dipolar character of the P=O group in phosphine oxides may be expected to have a significant influence on the structural properties of these materials, both with regard to short-range interactions (such as hydrogen bonding) and long-range electrostatic interactions (which may approximate to dipolar arrays of the P=O groups).

Although many hydrogen-bonded co-crystals of TPPO have been reported,[24, 28, 29, 32] these studies have focused on co-crystals based on N–H···O and O–H···O interactions, and only few cases involve significant C–H···O interactions.[30, 31] For this reason, we set out to explore systems in which C–H···O interactions may be formed with TPPO. As the P=O group is a good hydrogen-bond acceptor, a C–H···O interaction between TPPO and a good C–H donor (such as $CHCl_3$, $CH(NO_3)_3$, C≡C–H or NC–H) may be expected to produce short C–H···O contacts that are comparable in strength and geometric characteristics to traditional strong interactions such as O–H···O and N–H···O. As part of this work,[30] we investigated a co-crystal in which a $(TPPO)_2$–water aggregate, based on the hydrogen bonded P=O···H–O–H···O=P unit, forms an exceptionally short C–H···O hydrogen bond with a molecule of 1,4-diethynylbenzene (the C–H···O interaction involves a C≡C–H group of the 1,4-diethynylbenzene molecule as the donor and the oxygen atom of the water molecule (shown above) as the acceptor). In this aggregate, the polarization of the O–H bonds of the water molecule is promoted by the O–H···O=P interactions with the TPPO molecules, enhancing the negative polarization of the oxygen atom of the water molecule.

In order to explore systematically the factors that affect the structural properties of phosphine oxides in the solid state for cases in which no traditional strong hydrogen-bond donors are present, we focus here on the family of solid bis-diphenylphosphine oxides $(C_6H_5)_2PO(CH_2)_nPO(C_6H_5)_2$ (n = 1–8; **1**–**8**). For these molecules, two important intramolecular features are the conformation of the aliphatic $(CH_2)_n$ chain and the dependence of the relative orientations of the P=O dipoles on the chain length. The aliphatic chain prefers an all-*anti* conformation. For the compounds in which n is an even number (denoted the "even series"), the all-*anti* conformation leads to an antiparallel alignment of the two

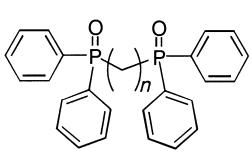

1 n = 1
2 n = 2
3 n = 3
4 n = 4
5 n = 5
6 n = 6
7 n = 7
8 n = 8

P=O groups in the molecule, whereas for the compounds in which n is an odd number (denoted the "odd series"), the all-*anti* conformation leads to a parallel alignment of the two P=O groups. For the even series, we may expect that the all-*anti* conformation should be adopted, as the antiparallel alignment of the P=O groups represents a favourable intramolecular dipolar interaction. However, for the odd series, the parallel alignment of the P=O groups leads to an unfavourable intramolecular electrostatic interaction, and becomes increasingly unfavourable as the aliphatic chain becomes shorter. For the odd series, it is clear that a compromise must be reached between the favourable all-*anti* conformation of the aliphatic chain (which forces the unfavourable parallel alignment of the P=O dipoles) and the avoidance of a parallel alignment of the P=O dipoles (which requires a distortion of the molecule from the favourable all-*anti* conformation of the aliphatic chain). The need to avoid a parallel alignment of the P=O dipoles may be particularly important for short aliphatic chains, which correspond to a shorter distance and stronger interaction between the two P=O dipoles in the molecule.

In understanding the crystal structures of these compounds, these intramolecular considerations must again be balanced against intermolecular factors, recognizing that different molecular conformations may be able to propagate different combinations of intermolecular interactions and to promote different three-dimensional packing arrangements. The bis-diphenylphosphine oxide molecules have four phenyl rings, and edge-to-face (C–H···π) and face-to-face (π···π) interactions, as well as C–H···O interactions, may have an important influence on the crystal packing. It is also important to consider the direct interactions between the P=O dipoles of different molecules, as these long-range electrostatic interactions may promote specific packing arrangements. In the present context, we recognize that, for a one-dimensional array of dipoles, a parallel co-axial arrangement provides the most favourable electrostatic interaction.

Results and Discussion

Preliminary remarks

The compounds in the odd series exhibit markedly different physical properties from those in the even series. For example, members of the odd series have good solubility in all solvents tested (toluene, benzene, acetone, chloroform, dichloromethane) whereas members of the even series are significantly soluble only in the halogenated solvents of those considered. Another property that differs markedly between the odd and even series is the melting temperature, which is substantially lower for the crystalline materials of the odd series than those

  0947-6539/00/0613-2339 $ 17.50+.50/0

of the even series (as discussed below, many of the crystalline materials of the odd series are actually solvates). In view of these observations and the discussion in the Introduction, it is reasonable to expect major differences in the structural properties between the even and odd series.

In the present work, the crystal structures of compounds **2**, **6** and **8** within the even series have been determined from single-crystal X-ray diffraction data, and relevant crystallographic data are summarized in Table 1. The crystal structure of **4** has been reported previously.[33] As discussed below in the section on the structural properties of the even series, there are strong similarities between the crystal structures of the compounds in the even series (particularly for **4**, **6** and **8**).

For the compounds in the odd series, only **7** was found to crystallize without the formation of a solvate co-crystal. For **3** and **5**, crystals suitable for single-crystal X-ray diffraction studies were obtained by crystallization from toluene, but were found to be solvate co-crystals with stoichiometries **3**·water and **5**·$(toluene)_2$. The **3**·water co-crystal was obtained reproducibly by crystallization from toluene, and presumably relies on residual amounts of water present in the solvent. In the present work, the crystal structures of **3**·water and **5**·$(toluene)_2$ have been determined from single-crystal X-ray diffraction data and the crystal structure of **7** has been determined directly from powder X-ray diffraction data. Relevant crystallographic data are summarized in Table 3. A solvate co-crystal of **1** with benzene (stoichiometry **1**·$(benzene)_{0.25}$) has been reported previously.[34] As the structural properties of these co-crystals are influenced not only by intrinsic characteristics of the bis-diphenylphosphine oxide molecules but also by the presence of the solvent molecules, it is not surprising that uniform structural behaviour in not observed across the set of crystal structures for the odd series. Nevertheless, certain aspects of these crystal structures contribute in a general sense to our understanding of the structural properties of bis-diphenylphosphine oxides, as discussed below in the section on the structural properties of the odd series.

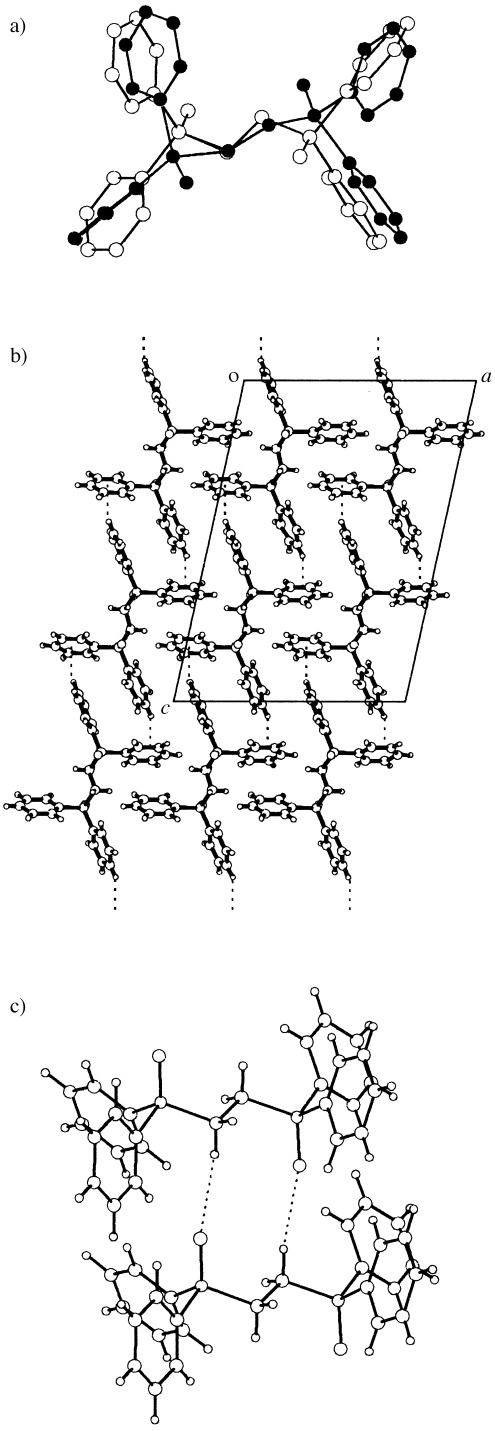

Figure 1. The crystal structure of **2** showing a) the asymmetric unit, b) the crystal packing arrangement viewed along the *b* axis (with C–H···π interactions shown by dotted lines) and c) short C–H···O contacts.

Structural properties of the even series

In the crystal structure of **2**, there is one molecule in the asymmetric unit. This molecule is disordered (Figure 1a; Table 1) between two orientations related approximately by 180° rotation about the long axis of the molecule (approximately the crystallographic *c* axis). The proportions of the two molecular orientations are 88.7% and 11.3%. From the average crystal structure, we cannot assess a priori whether the two molecular orientations represent two different ordered domains (situation A) or whether there is a uniform distribution (subject to the probabilities quoted above) of the two disordered molecular orientations throughout the crystal (situation B). Nevertheless, consideration of the intermolecular interactions discussed below strongly suggests that situation A, with ordered domains containing only the major orientation and ordered domains containing only the minor orientation, should be more favourable than situation B, in which individual molecules may adopt the minor orientation while surrounded by neighbouring molecules in the major orientation. The crystal structure for a domain comprising only the major orientation is shown in Figure 1b and is discussed below.

The $(CH_2)_2$ chain has the *anti* conformation, with the P=O groups in a given molecule oriented antiparallel to each other. In the crystal structure, P=O groups of neighbouring molecules are aligned approximately along the *b* axis (periodic repeat distance 5.8 Å), forming linear arrays of the type P=O···P=O···P=O, with O···P distances 4.34 Å and 4.39 Å

  0947-6539/00/0613-2340 $ 17.50+.50/0 *Chem. Eur. J.* **2000**, *6*, No. 13

Table 1. Crystallographic data for compounds in the even series.[a]

Compound	**2**	**4**	**6**	**8**
crystal system	monoclinic	triclinic	triclinic	triclinic
crystal size [mm^3]	$0.06 \times 0.08 \times 0.2$	–	$0.05 \times 0.2 \times 0.15$	$0.05 \times 0.2 \times 0.5$
space group	Cc	$P\bar{1}$	$P\bar{1}$	$P\bar{1}$
$R[I > 2\sigma(I)]$	0.111	–	0.0443	0.0594
wR_2	0.2381	–	0.1253	0.1443
a [Å]	16.308(4)	8.862(1)	8.865(7)	8.8029(14)
b [Å]	5.817(13)	12.517(2)	13.354(6)	14.123(2)
c [Å]	23.199(5)	5.826(1)	5.841(4)	5.9130(9)
α [°]	90	102.67(1)	101.42(2)	99.070(4)
β [°]	102.260(6)	104.22(1)	104.07(3)	104.602(7)
γ [°]	90	79.71(1)	83.52(3)	84.254(3)
V [Å^3]	2151(5)	592.5(3)	655.9(8)	701.1(2)
Z	4	1	1	1
ρ [g cm^{-3}]	1.329	1.285	1.227	1.219

[a] The data for **4** are taken from reference [33]. For **4**, the unit cell axes {a, b, c} shown above have been transformed from those {a_{pub}, b_{pub}, c_{pub}} quoted in reference [33] to facilitate comparison with the unit cells of **6** and **8**, with $a = b_{pub}$; $b = c_{pub}$; $c = a_{pub}$].

(for the two independent P=O groups) and P=O···P angles 167.3° and 165.9° respectively. These linear arrays are presumably mediated by electrostatic interactions between the P=O dipoles. For disorder situation B discussed above, molecules in the minor orientation would exist within an array of molecules of the major orientation, representing a defect (P=O···O=P···P=O) that is highly unfavourable on electrostatic grounds. On this basis, disorder model A appears more plausible than disorder model B, as discussed above. As shown in Figure 1c, there are also relatively short C–H···O=P interactions between neighbouring molecules along the b axis (involving aliphatic C–H bonds). Within the ac plane, neighbouring molecules interact through edge-to-face (C–H···π) interactions between phenyl rings. Of the four independent rings in a given molecule, two rings act as acceptors (π) for these interactions and two rings act as donors (C–H). The H···π(centroid) distances for these interactions are in the range 3.00 Å to 3.65 Å.

In summary, the crystal structure of **2** may be considered in terms of linear dipolar arrays of P=O···P=O interactions along the b axis, together with C–H···O interactions and C–H···π interactions. Distances and angles relating to these interactions are given in Table 2. There is no evidence for any significant π···π interactions between adjacent phenyl rings in this structure.

From inspection (see Table 1) of the unit cell dimensions for **4**, **6** and **8**, it is clear that these materials have strong structural similarities. As discussed below, these structures are essentially identical, except for the requirement to accommodate an extra $(CH_2)_2$ unit in the aliphatic chain on moving along the series (reflected mainly by a progressive increase in the length of the b axis) and a slight difference in the conformation of the aliphatic chain in the case of **8**. There are also some common features between the unit cell dimensions of **2** and those of **4**, **6** and **8**, suggesting some common packing motifs. For example, all structures in the even series have a unit cell axis of length about 5.8 Å (b axis for **2**; c axis for **4**, **6** and **8**). In view of the similar structural properties of **4**, **6** and **8**, we discuss these compounds together.

In the crystal structures of **4** (Figure 2), **6** (Figure 3) and **8** (Figure 4), the asymmetric unit comprises half the molecule, with the two halves of the molecule related by a centre of inversion at the mid-point of the central C–C bond. In **4** and **6**, the aliphatic chains have the all-*anti* conformation. In **8**, the majority of the aliphatic chain has the all-*anti* conformation, but with some deviation in the middle portion of the chain. In **4**, **6** and **8**, the two P=O groups in a given molecule are strictly antiparallel. The P=O groups of all molecules are aligned approximately along the c axis (periodic repeat distance ca. 5.8 Å), and the P=O groups of adjacent molecules form linear arrays of the type P=O···P=O···P=O. These arrays are presumably promoted by the favourable electrostatic interactions between the P=O dipoles. The geometrical characteristics of these arrays are remarkably constant for all members of the even series (including **2**), with O···P distances in the range 4.34 Å to 4.47 Å and P=O···P angles in the range 163.7° to 167.3° (see Table 2). In addition, adjacent molecules along the c axis are linked by C–H···O=P interactions (involving a C–H bond of the CH_2 group that is α with respect to the phosphine oxide group).

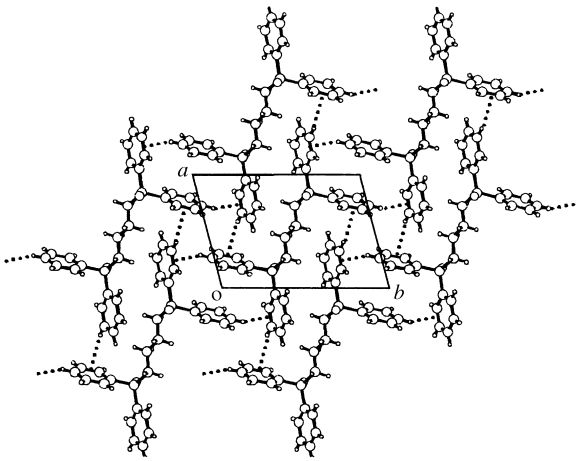

Figure 2. The crystal structure of **4** viewed along the c axis with short C–H···π contacts shown.

Table 2. Selected information on intermolecular interactions in the crystal structures of compounds in the even series.

Compound	C–H···O		P=O···P=O	
	C···O [Å]	C–H···O [°]	O···P [Å]	P=O···P [°]
2	3.60	169.4	4.39	165.9
	3.59	168.5	4.34	167.3
4	3.50	175.3	4.39	163.7
6	3.52	171.8	4.39	164.4
8	3.58	175.4	4.47	164.1

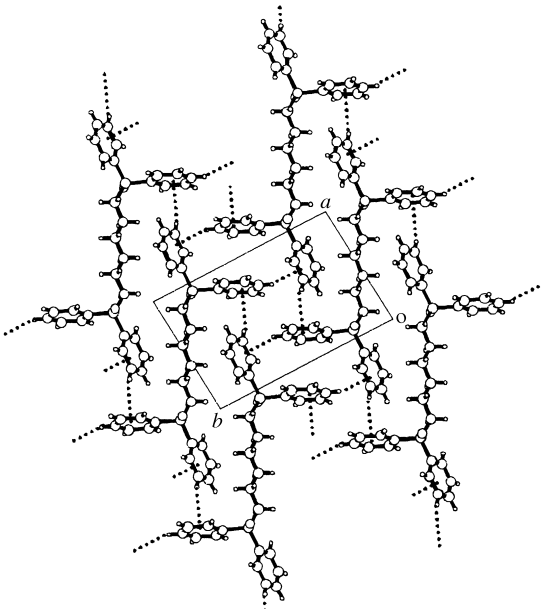

Figure 3. The crystal structure of **6** viewed along the *c* axis with short C–H···π contacts shown.

Each phenyl ring is involved in two edge-to-face (C–H···π) interactions with phenyl rings from different neighbouring molecules, in one case acting as the donor (C–H) and in the other case acting as the acceptor (π). In total, each molecule forms such interactions with four neighbours, giving rise to networks of C–H···π interactions in the *ab* plane (H···π(centroid) distances in the range 3.08 Å to 3.38 Å). There are no significant π···π interactions in any of the structures in the even series (pairs of phenyl rings that may appear in Figures 2, 3 and 4 to have π···π interactions are actually at different "heights" along the *c* axis).

In the crystal structure of **8**, the central part of the aliphatic chain is disordered between two different conformations, with 71.5% in the major component (Figure 4a). For both the major and minor components, the C-C-C-C dihedral angle for the C–C bond adjacent to the central C–C bond is approximately *gauche* (82° for the major component and 72° for the minor component) (note that the C-C-C-C dihedral angle for the next C–C bond away from the central C–C bond deviates slightly from *anti* (164° for the major component and 152° for the minor component)). The major and minor conformations differ only in the positions of the two central carbon atoms of the aliphatic chain, and all other atoms (including the diphenylphosphine oxide groups) are in identical positions. The C-C-C-C dihedral angle for the central C–C bond is 180° (as required by the fact that there is an inversion centre at the midpoint of this bond).

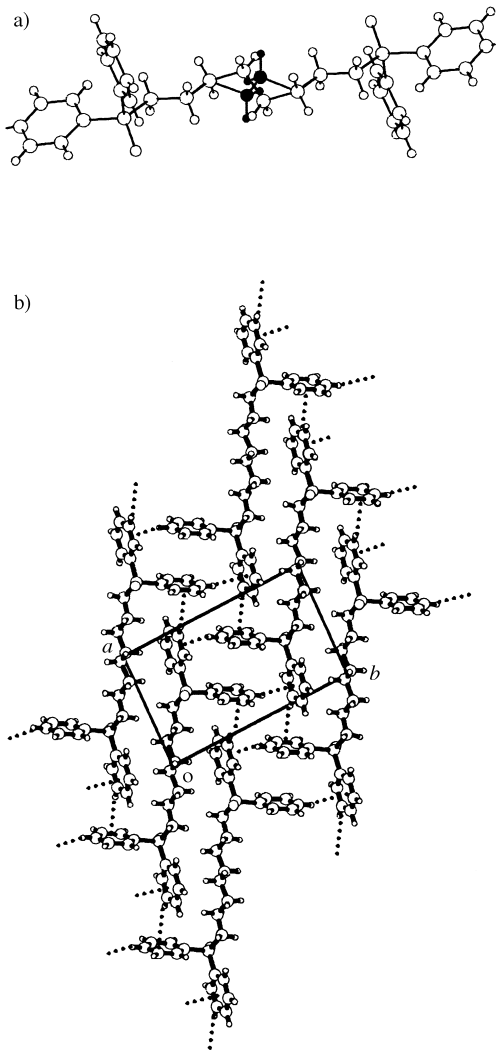

Figure 4. The crystal structure of **8** showing a) disorder in the molecular conformation and b) the packing arrangement for a domain comprising only the major component of the disordered structure, viewed along the *c* axis, with short C–H···π contacts shown.

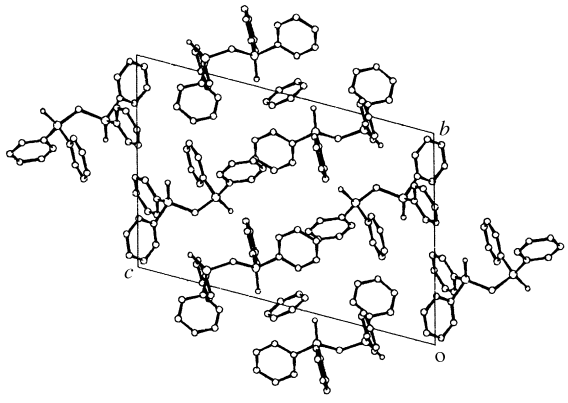

Figure 5. The crystal structure of **1**·(benzene)$_{0.25}$ viewed along the *a* axis.

Structural properties of the odd series

The crystal structure of **1**·(benzene)$_{0.25}$ (Figure 5; Table 3) has been reported previously.[34] The asymmetric unit comprises two molecules of **1** and half a molecule of benzene. For each molecule of **1** in the asymmetric unit, the P=O bonds within the molecule are almost antiparallel with O=P···P=O dihedral angles of 169.7° and 177.8°. In each molecule, two phenyl rings are almost parallel with perpendicular distances between the planes of about 3.24 Å and 3.27 Å. Several intermolecular edge-to-face (C–H···π) interactions are observed between molecules of **1**, with H···π(centroid) distances in the range 2.95 Å to 3.23 Å. In addition, the two

  0947-6539/00/0613-2342 $ 17.50+.50/0 *Chem. Eur. J.* **2000**, *6*, No. 13

Table 3. Crystallographic data for compounds in the odd series.[a]

Compound	**1**·(benzene)$_{0.25}$	**3**·water	**5**·(toluene)$_2$	**7**
crystal system	triclinic	monoclinic	monoclinic	monoclinic
crystal size [mm^3]	–	0.3 × 0.25 × 0.5	0.2 × 0.3 × 0.5	[b]
space group	$P\bar{1}$	$P2_1/a$	$P2_1/m$	$P2_1/n$
$R[I > 2\sigma(I)]$	–	0.0512	0.1438	[b]
wR_2	–	0.1602	0.3797	[b]
a [Å]	9.246(2)	7.920(2)	5.755(3)	12.560(1)
b [Å]	13.390(2)	19.484(8)	37.488(10)	10.203(1)
c [Å]	19.642(5)	15.582(7)	8.816(5)	22.889(2)
α [°]	74.14(2)	90	90	90
β [°]	78.42(2)	92.17(2)	102.80(5)	105.53(1)
γ [°]	84.59(2)	90	90	90
V [Å^3]	2290(2)	2403(2)	1855(2)	2826(1)
Z	4	4	2	4
ρ [g cm^{-3}]	1.265	1.278	1.174	1.176

[a] The data for **1**·(benzene)$_{0.25}$ are taken from reference [34]. [b] Structure determined from powder X-ray diffraction data ($R_p = 0.038$, $R_{wp} = 0.05$).

molecules of **1** in the asymmetric unit interact through C–H···O interactions involving C–H bonds of the CH_2 group. Each molecule of **1** has intramolecular C–H···O interactions (involving phenyl C–H), with C···O distances in the range 3.17 Å (C–H···O angle 173.9°) to 3.46 Å (C–H···O angle 166.5°). This structure does not contain any linear P=O···P=O···P=O dipolar arrays.

In the crystal structure of **3**·water (Figure 6), the asymmetric unit comprises one molecule of **3** and one molecule of water. The water molecules may be considered to occupy channels (along the *a* axis) formed by molecules of **3**. In the aliphatic chain, one C–C bond is *gauche* and the other C–C bond is *anti*, through which the two P=O bonds are brought towards an antiparallel alignment (O=P···P=O dihedral angle 148°). Ab initio calculations (HF/6-31G) indicate that the conformation observed in the crystal structure is more stable than the all-*anti* conformation (which contains parallel P=O dipoles) by 2.5 kcal mol^{-1}. For each molecule of **3** in the crystal structure, one P=O group points towards the water channel and participates in O–H···O hydrogen bonding with the water molecules to form hydrogen-bonded chains along the *a* axis (Figure 6b). In these arrays, each molecule of water is hydrogen-bonded to two P=O groups with approximately linear O–H···O interactions. The other P=O group in each molecule of **3** does not participate in hydrogen bonding. Short C–H···O contacts may also be identified between the oxygen atom of the water molecule and C–H bonds of two neighbouring phenyl rings, and between the oxygen atom of the water molecule and a C–H bond of the aliphatic chain. Interactions between different phenyl rings comprise both an edge-to-face (C–H···π) contact (H···π(centroid) distance 3.07 Å) and π···π interactions (perpendicular distance between planes ca. 3.6 Å; interfacial contact area ca. 1/3 of each ring). This structure does not contain any linear P=O···P=O···P=O dipolar arrays.

Crystals of **5**·(toluene)$_2$ were found to be unstable and it was necessary to keep the sample inside a sealed capillary during the single crystal X-ray diffraction measurement in order to avoid loss of solvent and consequent degradation of the crystal. The asymmetric unit comprises half a molecule of **5** and disordered toluene molecules (representing a total of one toluene molecule). The crystal structure is shown in Figure 7. The aliphatic chain has the all-*anti* conformation, with the P=O groups aligned essentially parallel to each other. The packing of the molecules of **5** creates two types of channel parallel to the *a* axis, which are occupied by toluene molecules. In one type of channel (denoted A), the channel walls are constructed only from phenyl rings (from four different molecules of **5** in the projection on the *bc* plane shown in Figure 7). In the other type

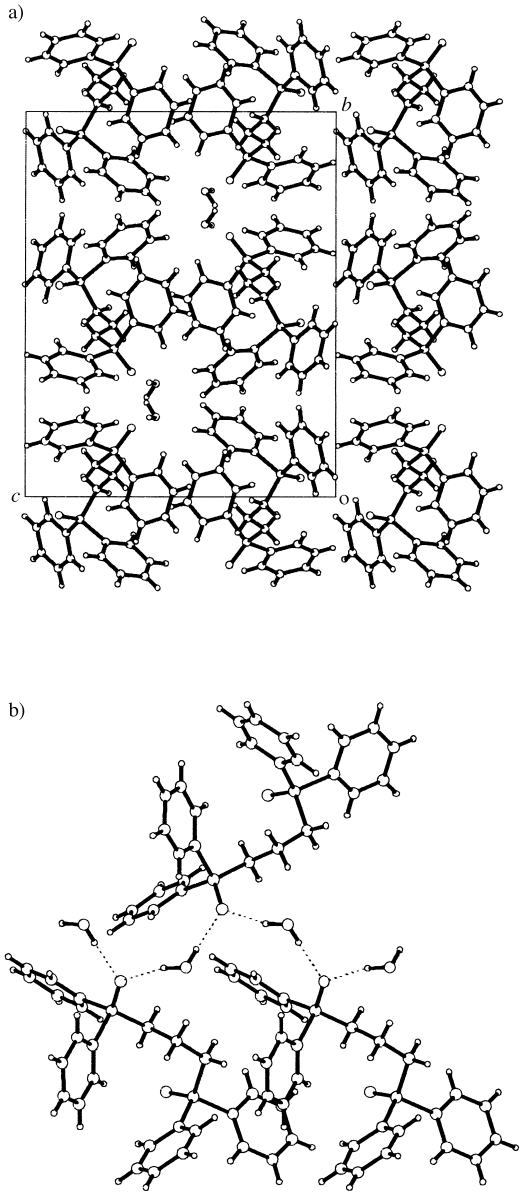

Figure 6. The crystal structure of **3**·water viewed along the *a* axis (the direction of the channel) (a) and showing the hydrogen-bonded chains along the *a* axis (horizontal) (b).

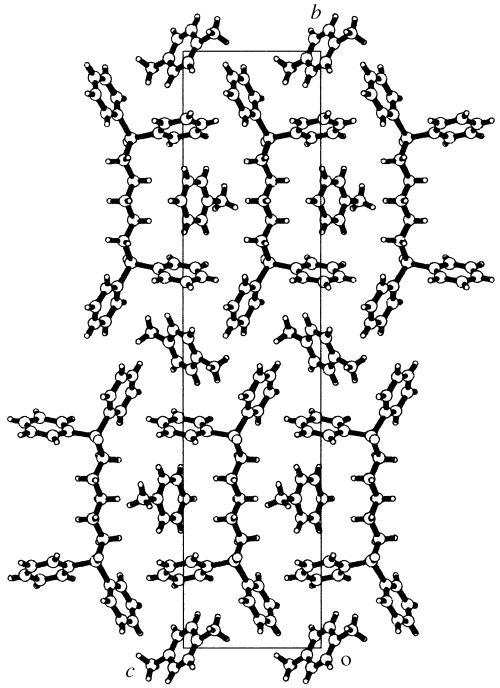

Figure 7. The crystal structure of **5**·(toluene)$_2$ viewed along the *a* axis (the direction of the channels). Some disordered toluene molecules have been omitted for clarity.

of channel (denoted B), the channel walls are constructed from the aliphatic chain and two phenyl rings of one molecule of **5** and the aliphatic chain of another molecule of **5** (as shown projected on the *bc* plane in Figure 7). In the channels of type A (which are rather elongated in cross-section), the toluene molecules are disordered with 50% occupancy between two orientations, with the same positions occupied by the carbon atoms of the phenyl rings of the two molecular orientations; the two methyl positions give rise to a "*p*-xylene-like" disordered molecule in the average structure. In the channels of type B, the toluene molecules are disordered with 50% occupancy between two orientations related by 180° rotation about the normal to the molecular plane; the positions of the carbon atoms of the phenyl rings of the two molecular orientations do not coincide in this case, although they are located in the same plane (for clarity, only one molecular orientation in the channels of type B is shown in Figure 7). The low stability of these crystals could be due to facile escape of the toluene molecules from the channels, leading to collapse of the host channel structure.

The structure of **5**·(toluene)$_2$ contains linear P=O···P=O···P=O dipolar arrays (O···P distance 4.32 Å; P=O···P angle 164.26°) along the *a* axis, directly analogous to those found in the crystal structures of compounds in the even series. This motif corresponds again to a characteristic unit cell axis of length about 5.8 Å. In addition, C–H···O interactions (C···O distance 3.48 Å; C–H···O angle 157.6°) may be identified between adjacent molecules along the *a* axis, as in the structures of the even series. Edge-to-face interactions are observed between the phenyl rings of adjacent molecules of **5** in the *bc* plane. Although the toluene molecules are disordered within their molecular planes, each molecule of **5** appears to act as the acceptor in C–H···π interactions from phenyl C–H bonds of toluene molecules in both channels (H···π(centroid) distances 3.37 Å and 3.54 Å) and to act as the donor in a C–H···π interaction to the toluene molecule in one channel (H···π(centroid) distance 3.31 Å). In the channels of type A, the methyl group of the toluene molecule is directed towards a phenyl ring of **5** (H···π(centroid) distance ca. 3.8 Å).

In the crystal structure of **7** (Figure 8a), the asymmetric unit comprises one molecule, which adopts a conformation with one *gauche* bond (C-C-C-C dihedral angle 57.7°) in the $(CH_2)_7$ chain and with the other bonds in this chain close to *anti*. This

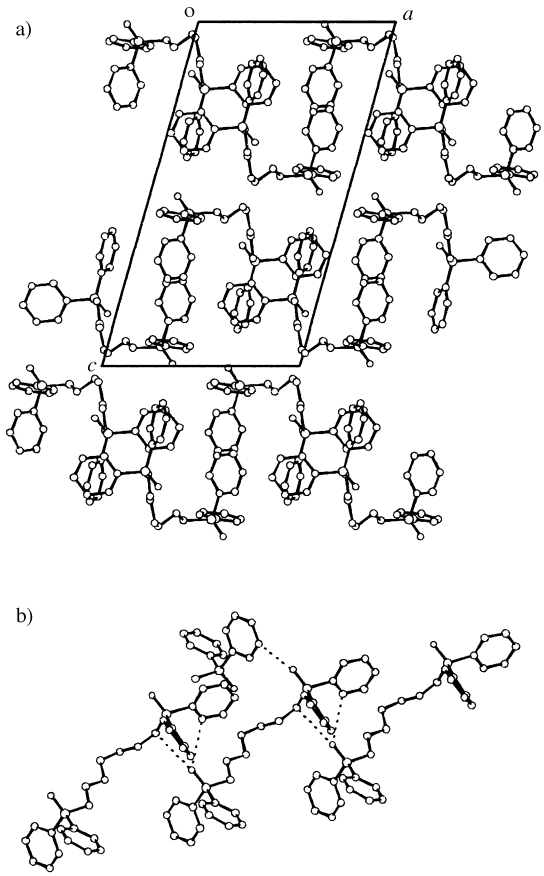

Figure 8. The crystal structure of **7** viewed along the *b* axis (a) and showing the short C–H···O contacts in the structure (b).

conformation of the $(CH_2)_7$ chain brings the two P=O groups in the molecule into almost parallel orientations (O=P···P=O dihedral angle 5.8°). As shown in Figure 8b, one P=O group is involved in two C–H···O interactions with a neighbouring molecule (involving one aliphatic C–H bond and one phenyl C–H bond), whereas the other P=O group is involved in one C–H···O interaction (with a phenyl C–H bond). The structure also contains several C–H···π interactions, but does not contain any linear P=O···P=O···P=O dipolar arrays.

Thermal analysis

The melting temperatures measured for all materials studied here are shown in Figure 9. We focus first on the structures that do not contain solvent molecules (i.e. the compounds in

  0947-6539/00/0613-2344 $ 17.50+.50/0 *Chem. Eur. J.* **2000**, *6*, No. 13

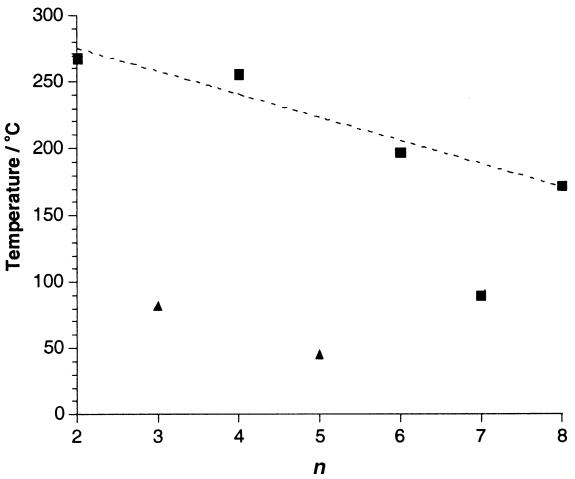

Figure 9. Measured melting temperatures (filled squares) for **2**, **4**, **6**, **7** and **8** and melting/decomposition temperatures (filled triangles) for **3**·water and **5**·(toluene)$_2$. The melting/decomposition behaviour for **3**·water and **5**·(toluene)$_2$ is discussed fully in the text (the temperatures shown correspond to loss of solvent from these crystal structures).

the even series (**2**, **4**, **6**, **8**) and **7**). In the even series, the melting temperature decreases (in a fairly linear manner) as *n* increases, and is mirrored by a gradual decrease in the density of the crystals as *n* increases. The melting temperature of **7** falls below the line established for the even series. For each of the compounds in the even series and **7**, the differential scanning calorimetry (DSC) thermogram shows only an endothermic process, which is assigned as the melting transition.

The melting behaviour of **3**·water and **5**·(toluene)$_2$ is less straightforward to define, as the first process that occurs on heating is decomposition of the co-crystal through loss of the included solvent molecules. Rapid heating on a melting point apparatus shows visible evidence of liquid at about 82 °C for **3**·water and at about 45 °C for **5**·(toluene)$_2$, probably corresponding to loss of solvent from these crystal structures. The resulting (de-solvated) solid phases melt subsequently at about 143 °C for **3** and at about 124 °C for **5** (only these transitions are observed under conditions of slow heating on a melting point apparatus).

On heating **3**·water in a thermogravimetric analysis (TGA) experiment, a total mass loss of 3.7% is observed, consistent with essentially complete loss of water (the theoretical amount of water in the crystal structure is 3.9%). This loss of water takes place in two steps, beginning (for heating rate 2 K min^{-1}) at about 55 °C (mass loss 2.0%) and at about 79 °C (mass loss 1.7%). DSC at heating rate 10 K min^{-1} shows a very broad endotherm beginning around 50 °C (presumably associated with the loss of water) followed by a sharp endotherm with onset at 140 °C (assigned as melting of the de-solvated solid phase of **3**). For **5**·(toluene)$_2$, TGA shows a similar two-step mass loss, with the total mass loss (25%) comparable to the theoretical amount of toluene (28%) in the crystal structure. At a heating rate of 2 K min^{-1}, the two mass losses begin at about 40 °C (8%) and about 55 °C (17%). DSC at a heating rate of 10 K min^{-1} shows two comparatively narrow exothermic peaks in the same temperature region (associated with the loss of toluene) followed by a sharp endotherm with onset at 124 °C (assigned as melting of the de-solvated solid phase of **5**).

Structural characterization of the materials obtained following removal of water from **3**·water and removal of toluene from **5**·(toluene)$_2$ represents an interesting area for future studies. An understanding of the phase behaviour of these materials (for example, on driving the solvent from the crystals and following the reintroduction of the same or different co-crystal molecules under controlled conditions) may reveal appropriate conditions for the preparation of unsolvated crystalline samples of **3** and **5** appropriate for structure determination from single crystal or powder diffraction data, allowing direct structural comparisons with the unsolvated crystal structures of the compounds in the even series and **7**. In addition it is relevant to note that, as demonstrated recently for another system,[46] de-solvated crystals produced in TGA experiments may be used as seeds for subsequent crystal growth of the de-solvated phase.

Solid-state NMR spectroscopy

It has been shown previously[35] that high-resolution solid-state ^{31}P NMR spectroscopy is a sensitive probe of the local structural properties of co-crystals containing triphenylphosphine oxide. In this light, we have extended our characterization of the structural properties of the bis-diphenylphosphine oxides **2**–**8** to include high-resolution solid-state ^{31}P NMR spectroscopy, allowing an assessment of the extent to which this technique is sensitive to the contrasts and similarities in the structural properties of the materials in this family.

The isotropic peaks in the high-resolution solid state ^{31}P NMR spectra of **2**, **3**·water, **4**, **5**·(toluene)$_2$, **6**, **7** and **8** are shown in Figure 10, and relevant data are summarized in Table 4. In general, the results are consistent with the crystal structures reported above. The high-resolution solid state ^{31}P NMR spectrum of **2** comprises two partially resolved peaks

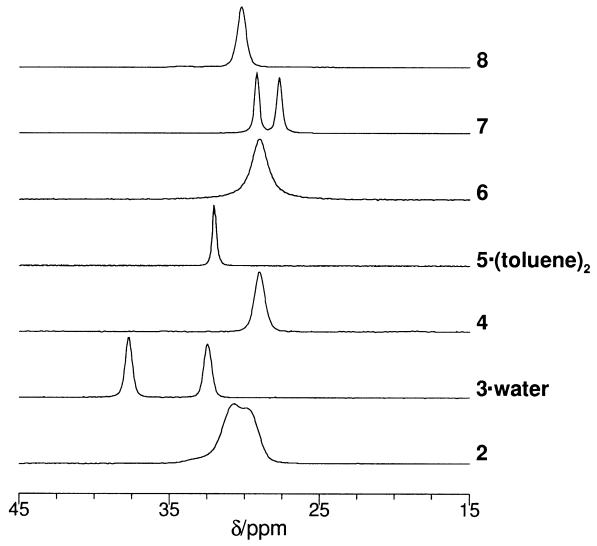

Figure 10. High-resolution solid-state ^{31}P NMR spectra for **2**, **3**·water, **4**, **5**·(toluene)$_2$, **6**, **7** and **8**.

  0947-6539/00/0613-2345 $ 17.50+.50/0

Table 4. Isotropic chemical shifts (δ), linewidths ($\Delta\nu$; full-width at half maximum) and relative integrated intensities (I) of the high-resolution solid-state ^{31}P NMR spectra of the bis-diphenylphosphine oxide materials studied. The linewidths and intensities for **2**, **3**·water and **7**, and the isotropic chemical shifts for **2**, were obtained by peak deconvolution.

Compound	**2**	**3**·water	**4**	**5**·(toluene)$_2$	**6**	**7**	**8**
δ [ppm]	30.9	32.4	29.1	32.1	29.0	29.2	30.3
	29.6	37.6				27.7	
$\Delta\nu$ [Hz]	185	100	75	39	156	49	85
I [%]	55	51	100	100	100	49	99
	45	49				51	

with approximately equal intensities, consistent with having one molecule of **2** (and thus two inequivalent ^{31}P nuclei) in the asymmetric unit. Some additional intensity is observed at $\delta \approx 32$, and may arise from the minor component in the disordered crystal structure. For **4**, **6** and **8**, the high-resolution solid-state ^{31}P NMR spectrum comprises a single isotropic peak, consistent with having one half molecule (i.e. one ^{31}P environment) in the asymmetric unit. The isotropic chemical shifts for **4**, **6** and **8** are similar, reflecting the similar local environments of the ^{31}P sites in the crystal structures. However, the slightly higher isotropic chemical shift for **8** in comparison with **4** and **6** is somewhat surprising in view of the very similar local structural properties in these materials. Nevertheless, the isotropic chemical shift for **8** is close to those for **2**, which also shares several local structural features in common with **4**, **6** and **8**.

The high-resolution solid-state ^{31}P NMR spectrum of **3**·water comprises two isotropic peaks separated by more than 5 ppm, consistent with having one molecule of **3** in the asymmetric unit. The significant separation between the peaks reflects significantly different local environments. The peak at $\delta = 37.6$ can be assigned to the ^{31}P site involved in P=O···H–O hydrogen bonding, as the formation of strong hydrogen bonds is known to shift isotropic ^{31}P resonances to higher frequency.[35] Indeed, the value of the isotropic chemical shift for this P=O group is entirely consistent with the value expected, according to the correlations developed previously,[35] for a P=O group engaged in two strong hydrogen bonds.

The single peak in the high-resolution solid-state ^{31}P NMR spectrum of **5**·(toluene)$_2$ is consistent with having one half molecule of **5** in the asymmetric unit. The isotropic chemical shift is significantly higher than those for compounds in the even series. We recall that **5**·(toluene)$_2$ and the compounds in the even series all exhibit P=O···P=O···P=O arrays, although other aspects of the crystal structures are substantially different, and are presumably responsible for the significant differences in isotropic chemical shifts.

The high-resolution solid state ^{31}P NMR spectrum of **7** contains two isotropic peaks, consistent with having one molecule of **7** in the asymmetric unit. The separation between these peaks (1.5 ppm) reflects significant differences, highlighted above, in the local interactions involving the two P=O groups in this structure.

The high-resolution solid state ^{31}P NMR spectra discussed above are clearly in good agreement with the known local structural properties of the materials studied. A more detailed understanding of the relationships between local structural properties and solid state NMR properties will focus on understanding the relationship between the anisotropy of the ^{31}P chemical shift tensor and local interactions involving the P=O group. The range of materials studied here, with their range of interactions and local structural situations involving P=O groups, provide a good opportunity for systematic fundamental studies in this area.

Conclusion

In summary, the bis-diphenylphosphine oxide compounds in the even series represent a systematic structural series, characterized by essentially linear P=O···P=O···P=O dipolar arrays (corresponding to a 5.8 Å unit cell axis), and augmented by C–H···O and C–H···π interactions. Compounds **4**, **6** and **8** in particular have virtually identical crystal structures. The persistence of the P=O···P=O···P=O dipolar arrays in these structures (and in the structure of **5**·(toluene)$_2$) emphasizes the important role that long range electrostatic interactions may play in influencing crystal structures, in addition to the much more localized types of interactions (such as hydrogen bonding) that are usually the focus of the structural rationalization and design of crystals.

In contrast, the compounds in the odd series do not exhibit uniform structural behaviour across the series, although these crystal structures nevertheless contribute to our general understanding of the structural properties of bis-diphenylphosphine oxides. The propensity for the compounds in the odd series (with the exception of **7**) to form solvate co-crystals alludes to the difficulties in forming crystal structures in which different packing factors are simultaneously optimized—clearly, the formation of co-crystals creates the opportunity for the formation of new types of interactions (such as O–H···O hydrogen bonding in the case of **3**·water) and new packing arrangements (such as the channel structure with linear P=O···P=O···P=O dipolar arrays in the case of **5**·(toluene)$_2$) which would otherwise not occur.

An important difference between the odd and even compounds concerns the molecular conformation. Thus, while the even compounds can (as observed in their crystal structures) adopt a conformation in which the favoured all-*anti* conformation of the aliphatic chain also corresponds to a favourable relative alignment of the two P=O dipoles in the molecule, this opportunity does not exist for the odd compounds. Thus, for the compounds in the odd series, the preferred all-*anti* conformation of the aliphatic chain gives rise to an unfavourable parallel alignment of the two P=O dipoles within the molecule, with the importance of avoiding a parallel alignment of the P=O dipoles becoming greater as the length of the aliphatic chain becomes shorter. This "frustration" with regard to the molecular conformation clearly complicates the formation of a well-defined structural series, particularly as the degree of frustration depends on chain length, and it is not surprising that different members of the odd series find different ways of relieving this frustration. In light of these facts, the contrasting thermal properties and

0947-6539/00/0613-2346 $ 17.50+.50/0 *Chem. Eur. J.* **2000**, *6*, No. 13

melting points (see section on thermal analysis and Figure 9) between the odd and even series is not surprising.

Finally, we note that for appropriate values of n, compounds in the family $(C_6H_5)_2PO(CH_2)_nPO(C_6H_5)_2$ are potential receptors (through the pair of P=O hydrogen bond acceptors) for "guest" molecules such as water and amines containing an appropriate pair of hydrogen bond donors. Binding of such molecules to the bis-diphenylphosphine oxides may be expected to occur in a highly selective manner, depending on the length (n) of the aliphatic chain, and may form the basis of selective molecular sensors. For such applications, the bis-diphenylphosphine oxide molecules may either be applied directly in the solid state or grafted on to appropriate substrates, with the further requirement that some appropriate physical property of the materials should vary in a well-defined manner as the concentration of bound species changes (corresponding to changes in the concentration of the "guest" molecules in the external environment). Clearly the fundamental understanding of structural properties of bis-diphenylphosphine oxides developed in the present paper represents an essential foundation upon which to design materials for such applications. We are currently exploring the potential of the bis-diphenylphosphine oxides with regard to such applications.

Experimental Section

Structure determination: Single crystals were grown by slow evaporation of solutions containing each of the bis-diphenylphosphine oxide compounds in a suitable solvent. Chloroform was used for **2**, **6** and **8**, toluene was used for **3** and **5**, and a dichloromethane/hexane mixture was used for **7**. All crystal structures with the exception of **7** were determined from single crystal X-ray diffraction data. Crystals of **7** suitable for conventional single crystal X-ray diffraction could not be grown, and the structure of **7** was determined instead from powder X-ray diffraction data.

Synchrotron microcrystal X-ray diffraction data were recorded for a microcrystal of **2** on station 9.8 at the SRS (Daresbury Laboratory), with $\lambda = 0.6875$ Å and using a Siemens SMART CCD detector and goniometer system. The crystal structure was solved by direct methods using the program SHELXS86 [36] and refined using SHELXL93. [37]

Single-crystal X-ray diffraction data for **3**·water, **5**·(toluene)$_2$ and **6** were recorded using graphite-monochromated $Cu_{K\alpha 1}$ radiation on a Rigaku R-Axis II diffractometer with rotating anode source and image plate detector. Data were recorded for two orientations of each crystal. In each orientation, image plate scans were recorded with crystal rotation in 10–15° frames about one axis over a total range of 180°. The crystal-to-detector distance was 55–76 mm and the exposure time was 30–50 minutes per frame. The same instrument was used to record single crystal X-ray diffraction data for **8**, but $Mo_{K\alpha}$ radiation was used and the image plate scans covered 180° with crystal rotation recorded in 4° frames. Data were processed using standard R-Axis II software.[38] The crystal structures were solved by direct methods[39] and refined using SHELXL93.[37]

The crystal structure of **7** was solved from powder X-ray diffraction data using the Genetic Algorithm method in our program GAPSS[40] and refined using standard Rietveld refinement techniques in the program GSAS.[41] Full details of this structure determination are described elsewhere.[42]

Powder X-ray diffraction patterns for **2**, **3**·water, **4**, **5**·(toluene)$_2$, **6**, **7** and **8** were recorded on a Siemens D5000 diffractometer using Ge-monochromated $Cu_{K\alpha 1}$ radiation and a linear position-sensitive detector covering 8° in 2θ. These powder diffraction patterns confirmed that, in all cases, the single crystals used for structure determination from single crystal diffraction data were representative of the bulk polycrystalline samples. Crystallographic data (excluding structure factors) for the structures reported in this paper have been deposited with the Cambridge Crystallographic Data Center as supplementary publication nos. CCDC-141361 (**2**), CCDC-141362 (**3**·water), CCDC-141363 (**5**·(toluene)$_2$), CCDC-141364 (**6**), and CCDC-141365 (**8**). Copies of the data can be obtained free of charge on application to CCDC, 12 Union Road, Cambridge CB2 1EZ, UK (fax: (+44) 1223-336-033; e-mail: deposit@ccdc.cam.ac.uk).

Thermal analysis: Differential scanning calorimetry (DSC) was carried out on a Perkin Elmer Pyris I instrument under helium purge and thermogravimetric analysis (TGA) was carried out using a Perkin Elmer TGA6 instrument under nitrogen. In both cases, the samples were heated at either 2 or 10 °C/min. Melting temperatures were determined using an Electrothermal 9200 melting point apparatus and are uncorrected.

Spectroscopy: Infrared spectra were recorded for ground polycrystalline samples dispersed in KBr disks, using a Perkin Elmer Paragon 1000 FT-IR spectrometer at ambient temperature with resolution 2 cm^{-1}. Solution state ^{1}H NMR spectra were recorded on a Bruker AC 300 (300 MHz) spectrometer using residual $CHCl_3$ present in deuterated chloroform as the internal reference. Solution-state ^{31}P NMR spectra were recorded on a Bruker AC 300 (121 MHz) spectrometer. Solution-state ^{13}C NMR spectra were recorded on a Bruker AC 300 (75 MHz) spectrometer using the PENDANT sequence. Mass spectra were recorded by using fast atom bombardment mass spectrometry on a VG ZabSpec mass spectrometer.

Solid-state NMR spectroscopy: High-resolution solid-state ^{31}P NMR spectra were recorded on a Chemagnetics CMX-Infinity 300 spectrometer (121.5 MHz) using either a Chemagnetics 3.2 mm double resonance probe or a 4 mm triple resonance probe. Cross-polarisation ($^{31}P \leftarrow {}^1H$), magic-angle sample spinning (MAS) and high-power ^{1}H decoupling were used. Typically the spinning frequency was (7000 ± 4) Hz and the decoupling field strength was about 62 kHz, with recycle delays in the range 30 s to 420 s. Chemical shifts are reported relative to the ^{31}P resonance in aqueous H_3PO_4 (85%) as an external standard. All spectra were recorded at 25 °C. Except in the case of **5**·(toluene)$_2$, all samples were ground to powders before loading into the zirconia rotors. The sample of **5**·(toluene)$_2$ was not ground, in view of the known susceptibility of this material to undergo decomposition by loss of toluene.

Synthesis: DMF was dried over 4 Å molecular sieves. THF was distilled from sodium/benzophenone and was used immediately. All other solvents and reagents were used as supplied. Thin-layer chromatography (TLC) was performed on aluminium plates coated with Merck Kieselgel 60 F_{254}. Flash column chromatography was performed using Kieselgel 60 (0.040–0.063 mm mesh Merk 9385).

Preparation of the hexa-P-phenyl-P,P′-alkyl-di-phosphonium bromides 9–15

General procedure: A mixture of the appropriate dibromoalkane (1 equiv) and triphenylphosphine (2 equiv) were heated under reflux for 10 h in dried DMF (50 mL). In a typical experiment, 5 g of the starting dibromide was used. The solvent was removed in vacuo and the products were recrystallised from CH_2Cl_2/hexane to afford colourless solids (55–86%).

Hexa-P-phenyl-P,P′-ethanediyl-bis-phosphonium bromide 9: Dibromoethane (5 g, 26.6 mmol) and triphenylphosphine (13.96 g, 53.2 mmol) afforded **9** (13.8 g, 73%). M.p. > 290 °C (from CH_2Cl_2/hexane); MS (FAB+): m/z (%): 633 ($[M-Br]^+$, 2), 475 (5), 289 (100), 262 (16), 183 (8); ^{1}H NMR (300 MHz; $CDCl_3$): $\delta = 4.20$ (d, $^2J_{P,H} = 4.4$ Hz, 4H; PCH_2), 7.62–7.82 (m, 18H; ArH), 7.95–8.08 (m, 12H; ArH); ^{13}C NMR (75 MHz; $CDCl_3$): $\delta = 56.7$ (PCH_2CH_2), 116.5 (d, $^1J_{P,C} = 87$ Hz; C1 Ph), 130.6, 134.6, 135.3.

Hexa-P-phenyl-P,P′-propanediyl-bis-phosphonium bromide 10: Dibromopropane (5 g, 24.7 mmol) and triphenylphosphine (12.98 g, 49.5 mmol) afforded **10** (11.7 g, 66%). M.p. > 290 °C (from CH_2Cl_2/hexane); MS (FAB+): m/z (%): 647 ($[M-Br]^+$, 17), 565 (6), 489 (10), 289 (100); ^{1}H NMR (300 MHz; $CDCl_3$): $\delta = 1.80-1.99$ (m, 2H, PCH_2CH_2), 4.54–4.73 (m, H, PCH_2), 7.52–8.05 (m, 30H, ArH); ^{13}C NMR (75 MHz; $CDCl_3$): $\delta =$ 17.7 (PCH_2CH_2), 22.3 (d, $^1J_{P,C} = 54.2$ Hz; PCH_2), 117.7 (d, $^1J_{P,C} = 87.4$ Hz, C1; Ph), 130.3 (d, $^2J_{P,C} = 6.0$ Hz; C2 and C2′ Ph), 134.0 (d, $^3J_{P,C} = 4.0$ Hz; C3 and C3′ Ph), 134.8 (C4 Ph).

Hexa-P-phenyl-P,P′-butanediyl-bis-phosphonium bromide 11: Dibromobutane (5 g, 23.1 mmol) and triphenylphosphine (12.1 g, 43.6 mmol) afforded **11** (10.7 g, 63%). M.p. > 290 °C (from CH_2Cl_2/hexane); MS (FAB+): m/z (%): 661 ($[M-Br]^+$, 55), 579 (52), 503 (24), 317 (77), 289

(100), 262 (58); ^{1}H NMR (300 MHz; $CDCl_3$): $\delta = 1.71-1.93$ (m, 4H; PCH_2CH_2), 3.62–3.85 (m, 4H; PCH_2), 7.68–8.02 (m, 30H; ArH); ^{13}C NMR (75 MHz; $CDCl_3$): $\delta = 22.0$ (d, $^1J_{P,C} = 51.3$ Hz; PCH_2), 23.1 (d, $^2J_{P,C} = 20.1$ Hz; PCH_2CH_2), 118.1 (d, $^1J_{P,C} = 86.1$ Hz, C1; Ph), 130.4 (d, $^2J_{P,C} = 12.6$ Hz; C2 and C2′ Ph), 134.1 (d, $^3J_{P,C} = 10.1$ Hz; C3 and C3′ Ph), 134.7 (C4 Ph).

Hexa-P-phenyl-P,P′-pentanediyl-bis-phosphonium bromide 12: Dibromopentane (5 g, 21.7 mmol) and triphenylphosphine (11.38 g, 43.4 mmol) afforded **12** (10.9 g, 67%). M.p. > 290 °C (from CH_2Cl_2/hexane); MS (FAB+): *m/z* (%): 675 ([*M* − Br]$^+$, 91), 593 (24), 517 (35), 331 (100), 289 (82), 262 (39); ^{1}H NMR (300 MHz; $CDCl_3$): $\delta = 1.75-2.25$ (m, 6H; $PCH_2CH_2CH_2$), 3.62–3.85 (m, 4H; PCH_2), 7.58–8.02 (m, 30H, ArH); ^{13}C NMR (75 MHz; $CDCl_3$): $\delta = 22.0$ ($PCH_2CH_2CH_2$), 22.6 (d, $^1J_{P,C} = 50.7$ Hz; PCH_2), 31.4 (d, $^2J_{P,C} = 17.5$ Hz; PCH_2CH_2), 118.2 (d, $^1J_{P,C} = 86.1$ Hz, C1; Ph), 130.4 (d, $^2J_{P,C} = 12.5$ Hz; C2 and C2′ Ph), 133.9 (d, $^3J_{P,C} = 9.9$ Hz; C3 and C3′ Ph), 134.8 (C-4).

Hexa-P-phenyl-P,P′-hexanediyl-bis-phosphonium bromide 13: Dibromohexane (6 g, 24.6 mmol) and triphenylphosphine (12.9 g, 49.2 mmol) afforded **13** (10.5 g, 55%). M.p. > 290 °C (from CH_2Cl_2/hexane); MS (FAB+): *m/z* (%): 689 ([*M* − Br]$^+$, 100), 607 (28), 531 (41), 345 (65), 289 (50), 262 (72); ^{1}H NMR (300 MHz; $CDCl_3$): $\delta = 1.54-1.95$ (m, 8H, $PCH_2(CH_2)_2$), 3.65–3.91 (m, 4H, PCH_2), 7.62–7.95 (m, 30H, ArH); ^{13}C NMR (75 MHz; $CDCl_3$): $\delta = 22.4$ (d, $^1J_{P,C} = 50.3$ Hz, PCH_2), 22.3 ($PCH_2CH_2CH_2$), 29.1 (d, $^2J_{P,C} = 16.4$ Hz, PCH_2CH_2), 118.2 (d, $^1J_{P,C} = 85.9$ Hz; C1 Ph), 130.5 (d, $^2J_{P,C} = 12.4$ Hz; C2 and C2′ Ph), 133.7 (d, $^3J_{P,C} = 9.8$ Hz; C3 and C3′ Ph), 134.9 (C4 Ph).

Hexa-P-phenyl-P,P′-heptanediyl-bis-phosphonium bromide 14: Dibromoheptane (2.88 g, 11.7 mmol) and triphenylphosphine (5.85 g, 22.3 mmol) afforded **14** (7.5 g, 86%). M.p. > 290 °C (from CH_2Cl_2/hexane); MS (FAB+): *m/z* (%): 703 ([*M* − Br]$^+$, 100), 621 (34), 545 (39), 359 (77), 311 (20), 289 (46); ^{1}H NMR (300 MHz; $CDCl_3$): $\delta = 1.52-2.08$ (m, 10H, $PCH_2(CH_2)_3$), 3.63–3.85 (m, 4H, PCH_2), 7.63–7.95 (m, 30H, ArH); ^{13}C NMR (75 MHz; $CDCl_3$): $\delta = 22.1$ (d, $^3J_{P,C} = 4.5$ Hz; $PCH_2CH_2CH_2$), 22.5 (d, $^1J_{P,C} = 50.3$ Hz; PCH_2), 27.3 ($PCH_2(CH_2)_2CH_2$), 29.6 (d, $^2J_{P,C} = 16.4$ Hz; PCH_2CH_2), 118.1 (d, $^1J_{P,C} = 85.9$ Hz; C1 Ph), 130.4 (d, $^2J_{P,C} = 12.4$ Hz; C2 and C2′ Ph), 133.7 (d, $^3J_{P,C} = 9.8$ Hz; C3 and C3′ Ph), 134.9 (C4 Ph).

Hexa-P-phenyl-P,P′-octanediyl-di-phosphonium bromide 15: Dibromooctane (1.55 g, 5.7 mmol) and triphenylphosphine (3 g, 11.4 mmol) afforded **15** (3.46 g, 76.3%). M.p. > 230 °C (from CH_2Cl_2/hexane); MS (FAB+): *m/z* (%): 717.2 ([*M*H − Br]$^+$, 100), 635 (43), 559 (41), 373 (41), 289 (53), 262 (73); ^{1}H NMR (300 MHz; $CDCl_3$): $\delta = 1.18-1.35$ (m, 4H; $P(CH_2)_3CH_2$), 1.52–1.75 (m, 8H, $PCH_2CH_2CH_2$), 3.54–3.78 (m, 4H, PCH_2), 7.61–7.95 (m, 30H; ArH); ^{13}C NMR (75 MHz; $CDCl_3$): $\delta = 22.3$ (d, $^3J_{P,C} = 3.0$ Hz; $P(CH_2)_2CH_2$), 22.7 (d, $^1J_{P,C} = 50.8$ Hz; PCH_2), 28.0 ($P(CH_2)_3CH_2$), 29.8 (d, $^2J_{P,C} = 16.4$ Hz; PCH_2CH_2), 118.2 (d, $^1J_{P,C} = 85.9$ Hz; C1 Ph), 130.5 (d, $^2J_{P,C} = 12.4$ Hz; C2 and C2′ Ph), 133.7 (d, $^3J_{P,C} = 10.2$ Hz; C3 and C3′ Ph), 135.0 (d, $^4J_{P,C} = 2.8$ Hz; C4 Ph).

Preparation of the tetra-P-phenyl-P,P′-alkenyl-bis-phosphine oxides 2–8

General procedure: The salt was heated under reflux for 10 h in 30% aqueous NaOH (50 mL). The mixture was cooled and diluted. The product was extracted with CH_2Cl_2 (2 × 20 mL). The organic layer was dried with $MgSO_4$ and filtered. The solvent was then removed under reduced pressure to afford colourless solids, that were recrystallised from CH_2Cl_2/hexane.

Tetra-P-phenyl-P,P′-ethanediyl-bis-phosphine oxide 2: Phosphonium bromide **9** (5 g, 6.9 mmol) and NaOH 30% (50 mL) afforded **2** (52.5 mg, 1.7% (low due to difficulties during purification)). M.p. 268.4–268.5 °C (from chloroform) (ref. 268–269 °C[43]); MS (FAB+): *m/z* (%): 453 ([*M*+Na]$^+$, 100), 431 ([*M*H]$^+$, 75), 229 (29), 176 (12), 154 (8); ^{1}H NMR (300 MHz; $CDCl_3$): $\delta = 2.50$ (d, $^2J_{P,C} = 2.5$ Hz, 4H; PCH_2), 7.39–7.56 (m, 12H; ArH), 7.64–7.75 (m, 8H; ArH); ^{13}C NMR (75 MHz; $CDCl_3$): $\delta = 21.6$ (d, $^1J_{P,C} = 74.1$ Hz; PCH_2), 128.8, 130.8, 131.1 (d, $^1J_{P,C} = 100.7$ Hz; C1 Ph), 132.1; ^{31}P NMR (121.5 MHz; solid-state CP MAS): $\delta = 30.7$; ^{31}P NMR (121.5 MHz; $CDCl_3$): $\delta = 32.9$.

Tetra-P-phenyl-P,P′-propanediyl-bis-phosphine oxide 3: Phosphonium bromide **10** (5 g, 6.8 mmol) and NaOH 30% (50 mL) afforded **3** (3 g, 98%). M.p. for **3**·water (crystallized from toluene) 142.9–143.2 °C (from slow heating), whereas fast heating resulted in the appearance of liquid at about 82 °C (see section on thermal analysis for a full discussion) (lit. 142–143 °C[44]); MS (FAB+): *m/z* (%): 445 ([*M*H]$^+$, 100), 367 (3), 307 (4), 201 (5), 154 (16); ^{1}H NMR (300 MHz; $CDCl_3$): $\delta = 1.90-2.11$ (m, 2H; PCH_2CH_2), 2.43–2.56 (m, 4H; PCH_2), 7.35–7.75 (m, 20H; ArH); ^{13}C NMR (75 MHz; $CDCl_3$): $\delta = 14.9$ (PCH_2CH_2), 30.2 (d, $^1J_{P,C} = 71.0$ Hz; PCH_2), 128.7 (d, $^2J_{P,C} = 10.8$ Hz; C2 and C2′ Ph), 130.7 (d, $^3J_{P,C} = 9.3$ Hz; C3 and C3′ Ph), 131.7 (C4 Ph), 132.7 (d, $^1J_{P,C} = 98.3$ Hz; C1 Ph); ^{31}P NMR (121.5 MHz; solid-state CP MAS): $\delta = 32.5$, 37.7; ^{31}P NMR (121.5 MHz; $CDCl_3$): $\delta = 32.7$.

Tetra-P-phenyl-P,P′-butanediyl-bis-phosphine oxide 4: Phosphonium bromide **11** (5 g, 6.7 mmol) and NaOH 30% (50 mL) afforded **4** (2.74 g, 88%). M.p. 256.2–256.6 °C (from chloroform) (lit. 259–260 °C[45]); MS (FAB+): *m/z* (%): 481 ([*M* + Na]$^+$, 100), 459 ([*M*H]$^+$, 53); ^{1}H (300 MHz; $CDCl_3$): $\delta = 1.62-1.81$ (m, 4H; PCH_2CH_2), 2.15–2.35 (m, 4H; PCH_2), 7.35–7.76 (m, 20H; ArH); ^{13}C NMR (75 MHz; $CDCl_3$): $\delta = 23.1$ (PCH_2CH_2), 29.5 (d, $^1J_{P,C} = 71.8$ Hz; PCH_2), 128.7 (d, $^2J_{P,C} = 11.6$ Hz; C2 and C2′ Ph), 130.7 (d, $^3J_{P,C} = 9.2$ Hz; C3 and C3′ Ph), 131.8 (C4 Ph), 132.8 (d, $^1J_{P,C} = 98.1$ Hz; C1 Ph); ^{31}P NMR (121.5 MHz; solid-state CP MAS): $\delta = 29.0$; ^{31}P NMR (121.5 MHz; $CDCl_3$): $\delta = 32.3$.

Tetra-P-phenyl-P,P′-pentanediyl-bis-phosphine oxide 5: Phosphonium bromide **12** (5 g, 6.6 mmol) and NaOH 30% (50 mL) afforded **5** (2.5 g, 78%). M.p. for **5**·(toluene)$_2$ (crystallized from toluene) 123.6–123.8 °C (from slow heating), whereas fast heating resulted in the appearance of liquid at about 45 °C (see section on thermal analysis for a full discussion) (lit. 124–126 °C[45]); MS (FAB+): *m/z* (%): 473 ([*M*H]$^+$, 100), 271 (5), 229 (4), 215 (7), 154 (5); ^{1}H NMR (300 MHz; $CDCl_3$): $\delta = 1.45-1.71$ (m, 6H; $PCH_2(CH_2)_2$), 2.12–2.28 (m, 4H; PCH_2), 7.35–7.85 (m, 20H; ArH); ^{13}C NMR (75 MHz;$CDCl_3$): $\delta = 20.9$ (PCH_2CH_2), 29.3 (d, $^1J_{P,C} = 71.9$ Hz; PCH_2), 31.9 ($PCH_2CH_2CH_2$), 128.6 (d, $^2J_{P,C} = 11.5$ Hz; C2 and C2′ Ph), 130.7 (d, $^3J_{P,C} = 9.1$ Hz; C3 and C3′ Ph), 131.7 (C4 Ph), 132.9 (d, $^1J_{P,C} = 97.9$ Hz; C1 Ph); ^{31}P NMR (121.5 MHz; solid-state CP MAS): $\delta = 32.1$; ^{31}P NMR (121.5 MHz; $CDCl_3$): $\delta = 33.8$.

Tetra-P-phenyl-P,P′-hexanediyl-bisphosphine oxide 6: Phosphonium bromide **13** (5 g, 6.5 mmol) and NaOH 30% (50 mL) afforded **6** (2.8 g, 89%). M.p. 196.9–197.2 °C (from chloroform) (lit. 196–198 °C[45]); MS (FAB+): *m/z* (%): 509 ([*M* + Na]$^+$, 67), 487 ([*M*H]$^+$, 32); ^{1}H NMR (300 MHz; $CDCl_3$): $\delta = 1.31-1.44$ (m, 4H; $PCH_2CH_2CH_2$), 1.48–1.66 (m, 4H; PCH_2CH_2), 2.13–2.27 (m, 4H; PCH_2), 7.38–7.76 (m, 20H; ArH); ^{13}C NMR (75 MHz; $CDCl_3$): $\delta = 21.3$ ($PCH_2CH_2CH_2$), 29.6 (d, $^1J_{P,C} = 72.2$ Hz; PCH_2), 30.5 (d, $^2J_{P,C} = 14.3$ Hz; PCH_2CH_2), 128.6 (d, $^2J_{P,C} = 11.5$ Hz; C2 and C2′ Ph), 130.7 (d, $^3J_{P,C} = 9.1$ Hz; C3 and C3′ Ph), 131.6 (C4 Ph), 133.0 (d, $^1J_{P,C} = 97.3$ Hz; C1 Ph); ^{31}P NMR (121.5 MHz; solid-state CP MAS): $\delta = 29.0$; ^{31}P NMR (121.5 MHz; $CDCl_3$): $\delta = 32.7$.

Tetra-P-phenyl-P,P′-heptanediyl-bis-phosphine oxide 7: Phosphonium bromide **14** (4 g, 5.1 mmol) and NaOH 30% (50 mL) afforded **7** (2.5 g, 98%). M.p. 90–91 °C (from CH_2Cl_2/hexane); MS (FAB+): *m/z* (%): 501 ([*M*H]$^+$, 100), 299 (6), 215 (6), 154 (11); ^{1}H NMR (300 MHz; $CDCl_3$): $\delta = 1.35-1.45$ (m, 6H, $PCH_2CH_2(CH_2)_2$), 1.55–1.70 (m, 4H; PCH_2CH_2), 2.13–2.28 (m, 4H, PCH_2), 7.40–7.79 (m, 20H; ArH); ^{31}C NMR (75 MHz; $CDCl_3$): $\delta =$ 21.3, 28.5, 29.6 (d, $^1J_{P,C} = 71.7$ Hz; PCH_2), 30.6 (d, $^2J_{P,C} = 14.7$ Hz; PCH_2CH_2), 128.6 (d, $^2J_{P,C} = 11.4$ Hz; C2 and C2′ Ph), 130.7 (d, $^3J_{P,C} =$ 9.1 Hz; C3 and C3′ Ph), 131.7 (C4 Ph), 133.1 (d, $^1J_{P,C} = 98.3$ Hz; C1 Ph); ^{31}P NMR (121.5 MHz; solid-state CP MAS): $\delta = 27.8$, 30.4; ^{31}P NMR (121.5 MHz; $CDCl_3$): $\delta = 32.9$.

Tetra-P-phenyl-P,P′-octanediyl-bis-phosphine oxide 8: Phosphonium bromide **15** (2 g, 2.5 mmol) and NaOH 30% (25 mL) afforded **8** (0.97 g, 75.9%). M.p. 172.4–172.8 °C (from chloroform) (lit. 170.5–172 °C[44]); MS (FAB+): *m/z* (%): 537 ([*M* + Na]$^+$, 100), 515 ([*M*H]$^+$, 39), 313 (9), 201 (10); ^{1}H NMR (300 MHz; $CDCl_3$): $\delta = 1.11-1.44$ (m, 8H; $P(CH_2)_2CH_2CH_2CH_2$), 1.45–1.68 (m, 4H; PCH_2CH_2), 2.12–2.36 (m, 4H; PCH_2), 7.32–7.84 (m, 20H; ArH); ^{13}C NMR (75 MHz; $CDCl_3$): $\delta = 21.3$ (d, $^3J_{P,C} = 3.96$ Hz, $PCH_2CH_2CH_2$), 28.7 ($P(CH_2)_3CH_2$), 29.6 (d, $^1J_{P,C} = 71.7$ Hz, PCH_2), 30.8 (d, $^2J_{P,C} = 14.7$ Hz), 128.6 (d, $^2J_{P,C} = 11.8$ Hz; C2 and C2′ Ph), 130.7 (d, $^3J_{P,C} = 9.6$ Hz; C3 and C3′ Ph), 131.6 (d, $^4J_{P,C} = 2.8$ Hz; C4 Ph), 133.1 (d, $^1J_{P,C} = 97.7$ Hz; C1 Ph); ^{31}P NMR (121.5 MHz; solid-state CP MAS): $\delta = 30.3$; ^{31}P NMR (121.5 MHz; $CDCl_3$): $\delta = 33.3$.

Acknowledgement

We are grateful to EPSRC, HEFCE and the University of Birmingham for financial support. Dr R L Johnston is thanked for his involvement in the

  0947-6539/00/0613-2348 $ 17.50+.50/0

work on structure solution from powder diffraction data, and Professor W. Clegg and Dr. S. Teat are thanked for assistance in connection with the microcrystal X-ray diffraction experiments on Station 9.8 at Daresbury Laboratory.

[1] C. B. Aakeroy, K. R. Seddon, *Chem. Soc. Rev.* **1993**, 397.
[2] G. R. Desiraju, *Angew. Chem.* **1995**, *107*, 2541; *Angew. Chem. Int. Ed. Engl.* **1995**, *34*, 2311.
[3] C. B. Aakeroy, *Acta Crystallogr. Sect. B* **1997**, *B53*, 569.
[4] G. R. Desiraju, *Chem. Commun.* **1997**, 1475.
[5] J. D. Dunitz, A. Gavezzotti, *Acc. Chem. Res.* **1999**, *32*, 677.
[6] L. Leiserowitz, *Acta Crystallogr. Sect. B* **1976**, *32*, 775.
[7] L. Leiserowitz, M. Tuval, *Acta Crystallogr. Sect. B* **1978**, *34*, 1230.
[8] Z. Berkovitch-Yellin, L. Leiserowitz, *J. Am. Chem. Soc.* **1980**, *102*, 7677.
[9] L. Leiserowitz, A. T. Hagler, *Proc. Royal Soc. A* **1983**, *388*, 133.
[10] M. C. Etter, *Acc. Chem. Res.* **1990**, *23*, 120.
[11] M. C. Etter, Z. Urbanczyk-Lipkowska, M. Zia-Ebrahimi, T. W. Panunto, *J. Am. Chem. Soc.* **1990**, *112*, 8415.
[12] M. C. Etter, S. M. Reutzel, *J. Am. Chem. Soc.* **1991**, *113*, 2586.
[13] F. Garcia-Tellado, S. J. Geib, S. Goswami, A. D. Hamilton, *J. Am. Chem. Soc.* **1991**, *113*, 9265.
[14] K. D. M. Harris, N. M. Stainton, A. M. Callan, R. A. Howie, *J. Mater. Chem.* **1993**, *3*, 947.
[15] J. C. MacDonald, G. M. Whitesides, *Chem. Rev.* **1994**, *94*, 2383.
[16] M. J. Krische, J. M. Lehn, N. Kyritsakas, J. Fisher, *Helv. Chim. Acta* **1998**, *81*, 1909.
[17] G. R. Desiraju, *Acc. Chem. Res.* **1996**, *29*, 441.
[18] J. Fawcett, A. W. G. Platt, D. R. Russel, *Inorg. Chim. Acta* **1998**, *274*, 177.
[19] I. Brassat, U. Englert, W. Keim, D. P. Keitel, S. Killat, G. Suranna, R. Wang, *Inorg. Chim. Acta* **1998**, *280*, 150.
[20] D. Thierbach, F. Huber, *Z. Anorg. Allg. Chem*. **1979**, *451*, 137.
[21] D. Thierbach, F. Huber, *Z. Anorg. Allg. Chem*. **1979**, *457*, 189.
[22] D. Thierbach, F. Huber, *Z. Anorg. Allg. Chem*. **1981**, *477*, 101.
[23] T. Gramstad, S. Husebye, K. Maartmann-Moe, *Acta Chem. Scand. Ser. B* **1986**, *40*, 26.
[24] M. C. Etter, P. W. Baures, *J. Am. Chem. Soc.* **1988**, *110*, 639.
[25] G. Ferguson, C. Glidewell, *J. Chem. Soc. Perkin Trans. 2* **1988**, 2129.
[26] G. Ferguson, C. Glidewell, A. J. Lough, *J. Chem. Soc. Perkin Trans. 2* **1989**, 2065.
[27] A. L. Llamas-Saiz, C. Foces-Foces, J. Elguero, P. Molina, M. Alajarin, A. Vidal, *J. Chem. Soc. Chem. Commun.* **1991**, 1694.
[28] D. E. Lynch, G. Smith, *Acta Crystallogr. Sect. C* **1993**, *49*, 285.
[29] D. E. Lynch, G. Smith, K. A. Briel, C. H. L. Kennard, A. K. Whittaker, J. V. Hanna, *Aust. J. Chem.* **1994**, *47*, 1401.
[30] B. M. Kariuki, K. D. M Harris, D. Philp, J. M. A. Robinson, *J. Am. Chem. Soc.* **1997**, *119*, 12679.
[31] T. Steiner, J. van der Maas, B. Lutz, *J. Chem. Soc. Perkin Trans. 2* **1997**, 1287.
[32] C. Lariucci, R. H. de Almeida Santos, J. R. Lechat, *Acta Crystallogr. Sect. C* **1986**, *42*, 1825.
[33] R. M. Fontes, G. Olivio, J. Zukerman-Schpector, S. L. Queiroz, A. A. Batista, *Acta Crystallogr. Sect. C* **1991**, *47*, 2699.
[34] M. Y. Antipin, Y. T. Struchkov, S. A. Pisareva, T. Y. Medved, *J. Struct. Chem*. **1980**, *21*, 644.
[35] S. Arumugam, C. Glidewell, K. D. M. Harris, *J. Chem. Soc. Chem. Commun.* **1992**, 724.
[36] G. M. Sheldrick, **1990**, SHELXS86, Program for Solution of Crystal Structures, University of Göttingen, Germany.
[37] G. M. Sheldrick, **1993**, SHELXL93, Program for the Refinement of Crystal Structures, University of Göttingen, Germany.
[38] Rigaku Corporation, **1994**, R-Axis II Software, Rigaku Corporation, Tokyo, Japan.
[39] Molecular Structure Corporation, **1993**, TEXSAN, Single Crystal Structure Analysis Software, Version 1.6, MSC, 3200 Research Forest Drive, The Woodlands, TX 77381, USA.
[40] K. D. M. Harris, R. L. Johnston, B. M. Kariuki, *Acta Crystallogr. Sect. A* **1998**, *54*, 632.
[41] A. C. Larson, R. B. Von Dreele, Los Alamos Lab. Report No. LA-UR-86–748, **1987**.
[42] B. M Kariuki, P. Calcagno, K. D. M. Harris, D. Philp, R. L. Johnston, *Angew. Chem.* **1999**, *111*, 860; *Angew. Chem. Int. Ed*. **1999**, *38*, 831.
[43] S. R. Postle, G. H. Whitham, *J. Chem. Soc. Perkin Trans. 1* **1977**, 2084.
[44] G. M. Kosolapoff, A. D. Brown, *J. Chem. Soc. C* **1967**, 1789.
[45] L. Horner, H. Hoffmann, W. Klink, H. Ertel, V. G. Toscano, *Chem. Ber.* **1962**, *95*, 581.
[46] D. Braga, G. Cojazzi, L. Maini, M. Polito, F. Grepioni, *Chem. Commun.* **1999**, 1949.

Received: October 8, 1999 [F2075]